Multifractal Processes

Rudolf H. Riedi[1]

Rice University, Dept. ECE, MS 366
6100 Main Street, Houston TX 77005 - 1892
email: riedi@rice.edu
Received May 16, 1999. Revised July 21, 1999[2]

Technical Report ECE Dept., Rice University, TR 99-06

Submitted for publication

Abstract

Multifractal theory up to date has been concerned mostly with random and deterministic singular measures, with the notable exception of fractional Brownian motion and Lévy motion. Real world problems involved with the estimation of the singularity structure of both, measures and processes, has revealed the need to broaden the known 'multifractal formalism' to include more sophisticated tools such as wavelets. Moreover, the pool of models available at present shows a gap between 'classical' multifractal measures, i.e. cascades in all variations with rich scaling properties, and stochastic processes with appealing statistical properties such as stationary increments, Gaussian marginals, and long-range dependence but with degenerate scaling characteristics.

This paper has two objectives, then. First, it develops the multifractal formalism in a context suitable for functions and processes emphasizing an intuitive approach. Binomial cascades and self-similar processes are treated extensively with a special eye on the use of wavelets. Second, it introduces truly multifractal processes, building a bridge between multifractal cascades and self-similar processes. Statistical properties of estimators as well as modeling issues are addressed but will appear elsewhere.

Keywords: Multifractal analysis, self-similar processes, fractional Brownian motion, Lévy flights, α-stable motion, wavelets, long-range dependence, multifractal subordination.

[1] Support comes from NSF grant no. MIP–9457438, ONR grant no. N00014–99–1–0813, and from Texas Instruments.

[2] This work was presented in part at the AMS meeting, Liousville, KT, March 1998, at the conference on 'Fractal Geometry and Statistics II' in Greifswald/Usedom, September 1998, and at the Summer school on 'Mathematics and Applications of Fractals' at the Newton Institute, Cambridge, January 1999.

1 Introduction and Summary

Fractal processes have a been successfully applied in various fields such as the theory of fully developed turbulence [6, 30, 48], stock market modeling [22, 51, 52], and more recently in the study of network data traffic [47, 58]. In networking, models using fractional Brownian motion (fBm) have helped advance the field through their ability of capturing fractal features such as statistical self-similarity and long-range dependence (LRD). It has been recognized, however, that multifractal features need to be accounted for towards a better understanding of network traffic, but also of stock exchange [28, 51, 66, 67, 72]. In short, there is a call for more versatile models which can, e.g., incorporate LRD and multifractal properties independently of each other.

Roughly speaking, a fractal entity is characterized by the inherent, ubiquitous occurrence of irregularities which governs its shape and complexity. The most prominent example is certainly fBm $B_H(t)$ [53]. Its paths are almost surely continuous but not differentiable. Indeed, the oscillation of fBm in any interval of size δ is of the order δ^H where $H \in (0,1)$ is the self-similarity parameter:

$$B_H(at) \stackrel{\text{fd}}{=} a^H B_H(t). \tag{1}$$

One reason for the success of fBm is that is uniquely defined through (1) and the fact that it is a Gaussian process. While (1) allows often for simple analysis, the fact of being Gaussian bears further advantages. The scaling property (1) implies also, according to [4], that fBm has a uniform oscillatory behavior (see Figure 1). Unfortunately, this comes as a disadvantage in various situations. Real world signals, as a matter of fact, often possess an erratically changing oscillation exponent (see Figure 2), limiting the appropriateness of fBm as a model. Due to the various exponents being present in such signals, they have been termed *multifractals*.

This paper has two objects. First, we present the framework for describing and detecting such a multifractal scaling structure. Doing so we survey local and global multifractal analysis and relate them via the multifractal formalism in a stochastic setting. Thereby, the importance of higher order statistics will become evident. It might be especially appealing to the reader to see wavelets put to novel use. We focus mainly on the analytical computation of the so-called multifractal spectra, and on their mutual relations, dwelling extensively on variations of binomial cascades. Statistical properties of estimators of multifractal quantities as well as modeling issues are addressed elsewhere (see [2, 32, 33] and [51, 65, 66]).

Second, we extend fBm to a process which is indeed multifractal: *Brownian motion in multifractal time*. This process has been suggested as a model for stock market exchange [51, 52] where oscillations are thought of as occurring in multifractal 'trading time'. The process seems also to appear naturally in Burgers equation with Brownian initial conditions [74, 82]. The reader interested in these multifractal processes may wish, at least at first reading, to content himself with the notation introduced on the following few pages, skip the sections which deal more carefully with the tools of multifractal analysis, and proceed directly to the last two sections. The remainder of this introduction provides a summary of the contents of the paper, following roughly its structure.

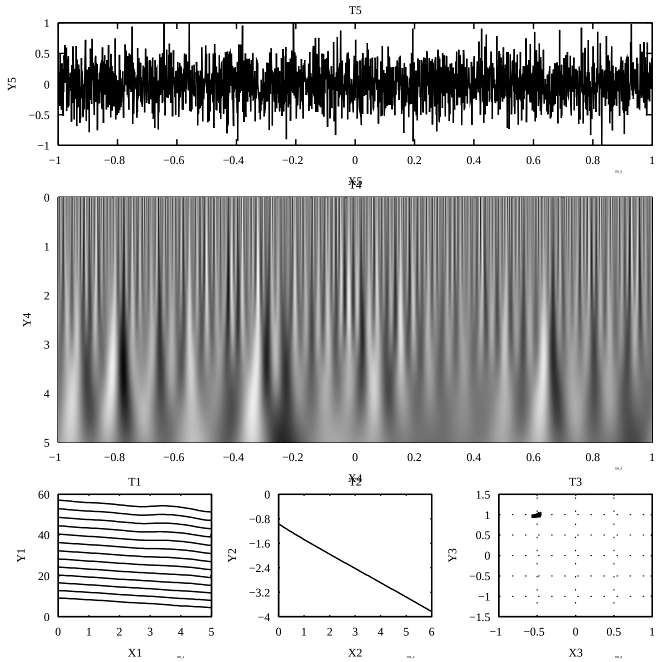

Figure 1: *Fractional Brownian motion, as well as its increment process called fGn (displayed on top in T5), has only one scaling exponent* $\underline{h}(t) = H$*, a fact which is represented in the linear partition function* τ *(see T2) and a multifractal spectrum (see T3) which consists of only one point: for fBm* $(H, 1)$ *and for fGn* $(H-1, 1)$*. For further details on the plots see (8), (5) and Figure 7.*

1.1 Singularity Exponents

In this work, we are mainly interested in the geometry or local scaling properties of the paths of a process $Y(t)$. Therefore, all notions and results concerning paths will apply to functions as well. For simplicity of the presentation we take $t \in [0, 1]$. Extensions to the real line $\mathbb{R}$ as well as to higher dimensions, being straightforward in most cases, are indicated.

A typical feature of a fractal process $Y(t)$ is that it has a non-integer degree of differentiability, giving rise to an interesting analysis of its local *Hölder exponent* $H(t)$. This $H(t)$ is the largest h such that $|Y(t') - P(t')| \le C|t' - t|^h$ for t' sufficiently close to t and for some polynomial P – the Taylor polynomial of Y at t.

Provided the polynomial is constant, $H(t)$ can be obtained using so-called *coarse Hölder exponents*, more precisely, $H(t) = \underline{h}(t)$ where

$$\underline{h}(t) = \liminf_{\varepsilon \to 0} h_\varepsilon(t) \qquad \text{where} \quad h_\varepsilon(t) = \frac{1}{\log \varepsilon} \log \sup_{|t'-t|<\varepsilon} |Y(t') - Y(t)|. \tag{2}$$

Vice versa, if $\underline{h}(t) \notin \mathbb{N}$ then $H(t) = \underline{h}(t)$ and the polynomial is indeed constant.

However, as the example $t^2 + t^{2.7}$ shows, the use of $\underline{h}(t)$ is ineffective in the presence of polynomial trends. Then, $\underline{h}(t)$ will reflect the lowest non-constant term of the Taylor

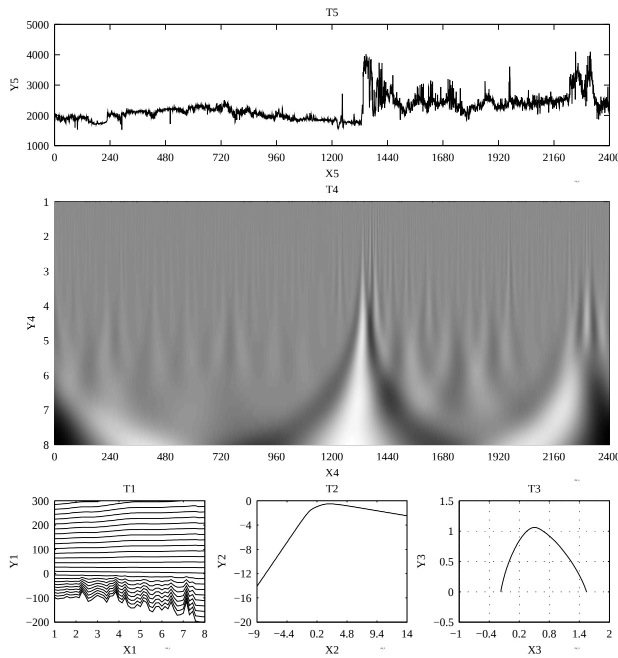

Figure 2: *Real world signals such as this geophysical data often exhibit erratic behavior and their appearance may make stationarity questionable. One such feature are 'trends' which, however, can be explained by strong correlations (LRD). Another one are sudden jumps or 'bursts' which in turn are a typical for multifractals. There, the scaling exponent* $\underline{h}(t)$ *depends erratically on time* t*, a fact which is reflected in the concave partition function* τ *(see T2) and a multifractal spectrum (see T3) which extends over a non-trivial range of scaling exponents. Both, LRD and multifractal processes may be stationary in some sense.*

polynomial of Y at t. For this reason, and also to avoid complications introduced through the computation of the supremum in (2), one may choose to employ *wavelet decompositions* or other tools of time frequency analysis. Properly chosen wavelets are blind to polynomials and due to their scaling properties they contain information on the Hölder regularity of Y [17, 40]. Their application in multifractal estimation has been pioneered by [6, 41]. Furthermore, wavelets provide unconditional basis for several regularity spaces such as Besov spaces (see (44) and (113)) whence their use bears further advantages.

Yet, the 'classical' choice of a singularity exponent is

$$\alpha_k^n = \frac{1}{-n \log 2} \log \left(\mathcal{M}((k+1)2^{-n}) - \mathcal{M}(k2^{-n}) \right). \tag{3}$$

It is attractive due to its simplicity and becomes actually quite powerful when studying monotonously increasing processes $\mathcal{M}(t)$, in particular the distribution functions of *singular measures*, such as cascades.

In the paper we will elaborate on the relation between these different singularity exponents.

1.2 Multifractal Spectra

As indicated we are mainly interested in the geometry or local regularity of the paths of $Y(t)$. Let us fix such a realization for the time-being.

1.2.1 Local analysis

Ideally, one would like to quantify in geometrical as well as statistical sense which values $\underline{h}(t)$ appear on a given path of the process Y, and how often one will encounter them. Towards the first description one studies the sets

$$E_a = \{t : \underline{h}(t) = a\} \tag{4}$$

The sets E_a form a decomposition of the support of Y according to its singularity exponents. We say that Y has a *rich multifractal structure* if these sets E_a are highly interwoven, each lying dense on the line. If so, only one of the E_a can have full Lebesgue measure, while the others form dusts, more precisely sets with non-integer Hausdorff dimension $\dim(E_a)$ [25]. Consequently, a *multifractal spectrum* can be defined as

$$d(a) := \dim(E_a). \tag{5}$$

In the 'classical' literature, $d(a)$ has been studied extensively as a compact representation of the complex singularity structure of Y.

To develop some intuition we note that the $d(a)$-spectrum of a differentiable path[3] reduces to the point $(1,1)$. On the other hand, if $\underline{h}(t)$ is continuous and not constant on intervals then each E_a is finite and $\dim(E_a) = 0$ for all a in the range of $\underline{h}(t)$. A spectrum $d(a)$ with non-degenerate form is, thus, indeed indication for rich singularity behavior. By this we mean that $\underline{h}(t)$ changes erratically with t and takes each value a on a rather large set E_a.

1.2.2 Global analysis

A simpler notion of a spectrum is obtained when adapting the concept of box-dimension to the multifractal context. As the name indicates, one aims at an estimate of $\dim(E_a)$ by counting the intervals – or boxes – over which Y increases roughly with the 'right' Hölder exponent. Therefore, we define the *grain (multifractal) spectrum* as [35, 36, 55, 68]

$$f(a) = \lim_{\varepsilon \to 0} \limsup_{n \to \infty} \frac{\log N^n(a, \varepsilon)}{n \log 2}, \tag{6}$$

where $N^n(a,\varepsilon) = \#\{k : |h_k^n - a| < \varepsilon\}$ counts the relevant grain exponents

$$h_k^n := -(1/n) \log_2 \sup\{|Y(s) - Y(t)| : (k-1)2^{-n} \le s \le t \le (k+2)2^{-n}\}. \tag{7}$$

This multifractal spectrum can be interpreted (at least) in three ways. First, as mentioned already it is related to the notion of *dimensions*. Indeed, a simple argument shows

[3] To avoid trivialities let us assume that this path and its derivative have no zeros.

that $\dim(E_a) \leq f(a)$ [70]. The essential ingredient for a proof is the fact that the calculation of $\dim(E_a)$ involves finding an optimal covering of E_a while $f(a)$ considers only uniform covers.

Second, (6) suggests that the *re-normalized histograms* $(1/n)\log_2 N^n(a,\varepsilon)$ should collapse at small scales 2^{-n}. For an ergodic process, one would at first glance hope to see the marginal distribution. However, the re-normalization implemented in $f(a)$ is aimed at detecting scaling properties which may cause most of the details of the marginal to be wiped out. Such is the case with fBm (1) where only the scaling parameter H contributes to $f(a)$, not the Gaussian density (see (139)). Consequently, fBm is 'mono-fractal' as mentioned above. To the contrary with multiplicative processes such as cascades, for which almost all details of the marginals may be reflected in f (see (108)).

The third natural context for the coarse spectrum f is that of Large Deviation Principles (LDP). Indeed, $N^n(a,\varepsilon)/2^n$ defines a probability distribution[4] on $\{h_k^n : k = 0,\ldots,2^n - 1\}$. Alluding to the Law of Large Numbers (LLN) we may expect this distribution to be concentrated more and more around the 'most typical' or 'expected' value as n increases. The spectrum $f(a)$ measures how fast the chance decreases to observe a 'deviant' value [23,68], i.e. $N^n(a,\varepsilon)/2^n \simeq 2^{f(a)-1}$.

1.3 Multifractal Formalism

The close connection to LDP leads one to study the scaling of 'sample moments' through the so-called *partition function* [30,35,36,68]

$$\tau_h(q) := \liminf_{n\to\infty} \frac{\log S_h^n(q)}{-n\log 2} \qquad \text{where} \quad S_h^n(q) := \sum_{k=0}^{2^n-1} 2^{-nqh_k^n}. \tag{8}$$

Similarly, replacing h_k^n by α_k^n, one defines $\tau_\alpha(q)$ and $S_\alpha^n(q)$ which takes on the well-known form of a partition sum

$$S_\alpha^n(q) = 2^{-nq\alpha_k^n} = \sum_{k=0}^{2^n-1} \left|Y\left((k+1)2^{-n}\right) - Y(k2^{-n})\right|^q \tag{9}$$

If the choice h_k^n or α_k^n does not matter we simply drop the index.

1.3.1 A Large Deviation Principle

The theory of LDP suggests $f(a)$ and $\tau(q)$ are strongly related since $2^{-n}S^n(q)$ is the moment generating function of the random variable $A_n(k) := -nh_k^n\ln(2)$ (recall footnote 4). For a motivativion of a formula consider the heuristics

$$S^n(q) \;=\; \sum_a \sum_{h_k^n\simeq a} 2^{-nqh_k^n} \simeq \sum_a 2^{nf(a)}2^{-nqa} = \sum_a 2^{-n(qa-f(a))} \simeq 2^{-n\inf_a(qa-f(a))}.$$

Making this argument rigorous we prove in this paper that

$$\tau(q) = f^*(a) := \inf_a(qa - f(a)). \tag{10}$$

[4] Recall that we fixed a path of Y. Randomness is here understood in choosing k.

Here $(\cdot)^*$ denotes the Legendre transform which is omnipresent in the theory of LDP. Indeed, by applying a theorem due to Gärtner and Ellis [21] and imposing some regularity on $\tau(q)$ theorem 5 shows that the family of probability densities defined by $N^n(a,\varepsilon)/2^n$ satisfies the *full LDP [20] with rate function* f meaning that f is actually a double-limit and $f(a) = \tau^*(a)$. Corollary 18 establishes that always

$$f(a) = \tau^*(a) = qa - \tau(q) \qquad \text{at points } a = \tau'(q). \tag{11}$$

Going through some of the explicitly calculated examples in Section 5.4 will help de-mystify the Legendre transform.

From (10) follows, that $f(a) \le f^{**}(a) = \tau^*(a)$ and also that $\tau(q)$ is a concave function, hence continuous and almost everywhere differentiable.

1.3.2 Deterministic envelop

So far, all that has been said applies to any given function or path of a process. In the random case, one would often like to use an analytical approach in order to gain intuition or an estimate of f for a typical path of Y.

To this end we formulate a LDP for the sequence of distributions of $\{h_k^n\}$ where randomness enters now through choosing $k \in \{0, \ldots, 2^n - 1\}$ as well as through the randomness of the process itself, i.e. through $Y_t(\omega)$ where ω lies in the probability space (Ω, P_Ω). The moment generating function of $A_n(k,\omega) = -nh_k^n(\omega)\ln(2)$ with k and ω random is $2^{-n}\mathbb{E}_\Omega[S^n(q)]$. This leads to defining the 'deterministic envelop':

$$T(q) := \liminf_{n\to\infty} \frac{-1}{n} \log_2 \mathbb{E}_\Omega S^n(q) \tag{12}$$

and the corresponding 'rate function' F (see (67)). As with the pathwise $f(a)$ and $\tau(q)$ we have here again $T(q) = F^*(q)$. More importantly, it is easy to show that $\tau(q,\omega) \ge T(q)$ almost surely (see lemma 8). Thus:

Corollary 1 *With probability one the multifractal spectra are ordered as follows: for all a*

$$\dim(E_a) \le f(a) \le \tau^*(a) \le T^*(a). \tag{13}$$

Great effort has been spent on investigating under which assumptions equality holds between some of the spectra, say between $\dim(E_a)$ as defined in terms of $\underline{h}(t)$ and $\tau^*(a)$ as obtained from a wavelet transform of Y. It has become the accepted term in the literature to say that *the multifractal formalism holds* if any such relation exists. Not indicating the nature of the parts of such an equality we find this terminology sometimes confusing and prefer to call (13) *the multifractal formalism*: this formula 'holds' for any choice of a singularity exponent as is shown in the paper.

1.4 Self-similarity and LRD

The statistical self-similarity as expressed in (1) makes fBm, or rather its increment process a paradigm of *long range dependence* (LRD). To be more explicit let δ denote some fixed lag and define *fractional Gaussian noise* (fGn) as

$$G(k) := B_H((k+1)\delta) - B_H(k\delta). \tag{14}$$

Having the LRD property means that the auto-correlation $r_G(k) := \mathbb{E}_\Omega[G(n+k)G(n)]$ decays so slowly that $\sum_k r_G(k) = \infty$. The presence of such strong dependence bears an important consequence on the aggregated processes

$$G^{(m)}(k) := \frac{1}{m} \sum_{i=km}^{(k+1)m-1} G(i). \tag{15}$$

They have a much higher variance, and variability, than would be the case for a short range dependent process. Indeed, if $X(k)$ are i.i.d., then $X^{(m)}(k)$ has variance $(1/m^2)\text{var}(X_0 + \ldots + X_{m-1}) = (1/m)\text{var}(X)$. For G we find, due to (1) and $B_H(0) = 0$,

$$\text{var}(G^{(m)}(0)) = \text{var}\left(\frac{1}{m}B_H(m\delta)\right) = \text{var}\left(\frac{m^H}{m}B_H(\delta)\right) = m^{2H-2}\text{var}\left(B_H(\delta)\right). \tag{16}$$

For $H > 1/2$ this expression decays indeed much slower than $1/m$. As is shown in [14] $\text{var}(X^{(m)}) \simeq m^{2H-2}$ is equivalent to $r_X(k) \simeq k^{2H-2}$ and so, $G(k)$ is indeed LRD for $H > 1/2$ (this follows also directly from (132)).

Let us demonstrate with fGn how to relate LRD with multifractal analysis using only that it is a zero-mean processes, not (1). To this end let $\delta = 2^{-n}$ denote the finest resolution we will consider, and let 1 be the largest. For $m = 2^i$ $(0 \leq i \leq n)$ the process $mG^{(m)}(k)$ becomes simply $B_H((k+1)m\delta) - B_H(km\delta) = B_H((k+1)2^{i-n}) - B_H(k2^{i-n})$. But the second moment of this expression —which is also the variance— is exactly what determines $T_\alpha(2)$ (compare (9)). More precisely, using stationarity of G and substituting $m = 2^i$, we get

$$2^{-(n-i)T_\alpha(2)} \simeq \mathbb{E}_\Omega\left[S_\alpha^{n-i}(2)\right] = \sum_{k=0}^{2^{n-i}-1} \mathbb{E}_\Omega\left[|mG^{(m)}(k)|^2\right] = 2^{n-i}2^{2i}\text{var}\left(G^{(2^i)}\right). \tag{17}$$

This should be compared with the definition of the LRD-parameter H via

$$\text{var}(G^{(m)}) \simeq m^{2H-2} \qquad \text{or} \qquad \text{var}(G^{(2^i)}) = 2^{i(2H-2)}. \tag{18}$$

At this point a conceptual difficulty arises. Multifractal analysis is formulated in the limit of small scales ($i \to -\infty$) while LRD is a property at large scales ($i \to \infty$). Thus, the two exponents H and $T_\alpha(2)$ can in theory only related when assuming that the scaling they represent is actually exact at all scales, and not only asymptotically.

In any real world application, however, one will determine both, H and $T_\alpha(2)$, by finding a *scaling region* $\underline{i} \leq i \leq \overline{i}$ in which (17) and (18) hold up to satisfactory precision. Comparing the two scaling laws in i yields $T_\alpha(2) + 1 - 2 = 2H - 2$, or

$$H = \frac{T_\alpha(2) + 1}{2}. \tag{19}$$

This formula expresses most pointedly, how *multifractal analysis goes beyond second order statistics*: in (28) we compute with $T(q)$ the scaling of *all* moments. The relation (19), here derived for zero-mean processes, can be put on more solid grounds using wavelet estimators of the LRD parameter [3] which are more robust than the ones through variance. The same formula (19) reappears also for multifractals (see (29) and (153)), suggesting that it has some 'universal truth' to it.

1.5 Multifractal Processes

The most prominent examples where one finds coinciding, strictly concave multifractal spectra are the distribution functions of *cascade* measures [5,11,26,38,43,48,59,63,68,71] for which $\dim(E_a)$ and $T^*(a)$ are equal and have the form of a $\cap$ (see Figure 6 and also 3 (e)). These cascades are constructed through some multiplicative iteration scheme such as the Binomial cascade, which is presented in detail in the paper with special emphasis on its wavelet decomposition. Having positive increments, this class of processes is, however, sometimes too restrictive. fBm, as noted, has the disadvantage of a poor multifractal structure and does not contribute to a larger pool of stochastic processes with multifractal characteristics.

It is also notable that the first 'natural', truly multifractal stochastic process to be identified was Lévy motion [42]. This example is particularly appealing since scaling is not injected into the model by an iterative construction (this is what we mean by the term natural). However, its spectrum is, though it shows a non-trivial range of scaling exponents $h(t)$, degenerated in the sense that it is linear.

1.5.1 Construction and Simulation

With the formalism presented here, the stage is set for constructing and studying new classes of truly multifractional processes. The idea, to speak in Mandelbrot's own words, is inevitable after the fact. The ingredients are simple: a multifractal 'time warp', i.e. an increasing function or process $\mathcal{M}(t)$ for which the multifractal formalism is known to hold, and a function or process V with strong mono-fractal scaling properties such as *fractional Brownian motion* (fBm), a Weierstrass process or self-similar martingales such as Lévy motion. One then forms the compound process

$$\mathcal{V}(t) := V(\mathcal{M}(t)). \tag{20}$$

To build an intuition let us recall the method of *midpoint displacement* which can be used to define simple Brownian motion $B_{1/2}$ which we will also call *Wiener motion* (WM) for a clear distinction from fBm. This method constructs $B_{1/2}$ iteratively at dyadic points. Having constructed $B_{1/2}(k2^{-n})$ and $B_{1/2}((k+1)2^{-n})$ one defines $B_{1/2}((2k+1)2^{-n-1})$ as $(B_{1/2}(k2^{-n}) + B_{1/2}((k+1)2^{-n}))/2 + X_{k,n}$. The off-sets $X_{k,n}$ are independent zero mean Gaussian variables with variance such as to satisfy (1) with $H = 1/2$. Thus the name of the method. One way to obtain *Wiener motion in multifractal time* WM(MF) is then to keep the off-set variables $X_{k,n}$ as they are but to apply them at the time instances $t_{k,n}$ defined by $t_{k,n} = \mathcal{M}^{-1}(k2^{-n})$, i.e. $\mathcal{M}(t_{k,n}) = k2^{-n}$:

$$\mathcal{B}_{1/2}(t_{2k+1,n+1}) := \frac{\mathcal{B}_{1/2}(t_{k,n}) + \mathcal{B}_{1/2}(t_{k+1,n})}{2} + X_{k,n}. \tag{21}$$

This amounts to a *randomly located random displacement*, the location being determined by $\mathcal{M}$. Indeed, (20) is nothing but a time warp.

An alternative construction of 'warped Wiener motion' WM(MF) which yields an equally spaced sampling as opposed to the samples $\mathcal{B}_{1/2}(t_{k,n})$ provided by (21) is desirable.

To this end, note first that the increments of WM(MF) become independent Gaussians once the path of $\mathcal{M}(t)$ is realized. To be more precise, fix n and let

$$\mathcal{G}(k) := \mathcal{B}((k+1)2^{-n}) - \mathcal{B}(k2^{-n}) = B_{1/2}(\mathcal{M}(k+1)2^{-n})) - B_{1/2}(\mathcal{M}(k2^{-n})). \tag{22}$$

For a sample path of $\mathcal{G}$ one starts by producing first the random variables $\mathcal{M}(k2^{-n})$. Once this is done, the $\mathcal{G}(k)$ simply are independent zero-mean Gaussian variables with variance $|\mathcal{M}(k+1)2^{-n})) - \mathcal{M}(k2^{-n})|$. This procedure has been used in Figure 3.

1.5.2 Global analysis

For the right hand side (RHS) of the multifractal formalism (13), we need only to know that V is an H-sssi process, i.e. that the increment $V(t+u) - V(t)$ is equal in distribution to $u^H V(1)$ (compare (1)). Assuming independence between V and $\mathcal{M}$ a simple calculation reads as

$$\begin{aligned} &\mathbb{E}_\Omega \sum_{k=0}^{2^n-1} |\mathcal{V}((k+1)2^{-n}) - \mathcal{V}(k2^{-n})|^q \\ &= \sum_{k=0}^{2^n-1} \mathbb{E}\mathbb{E}\left[|V(\mathcal{M}((k+1)2^{-n})) - V(\mathcal{M}(k2^{-n}))|^q \,\middle|\, \mathcal{M}(k2^{-n}), \mathcal{M}((k+1)2^{-n})\right] \\ &= \sum_{k=0}^{2^n-1} \mathbb{E}\left[|\mathcal{M}((k+1)2^{-n}) - \mathcal{M}(k2^{-n})|^{qH}\right] \mathbb{E}\left[|V(1)|^q\right]. \end{aligned} \tag{23}$$

With little more effort the increments $|\mathcal{V}((k+1)2^{-n}) - \mathcal{V}(k2^{-n})|$ can be replaced by suprema, i.e. by $2^{-nh_k^n}$, or even certain wavelet coefficients under appropriate assumptions (see theorem 38). It follows that

$$\text{Warped } H\text{-sssi:} \qquad T_\mathcal{V}(q) = \begin{cases} T_\mathcal{M}(qH) & \text{if } \mathbb{E}_\Omega\left[|\sup_{0\le t\le 1} V(t)|^q\right] < \infty \\ -\infty & \text{else.} \end{cases} \tag{24}$$

Simple H-sssi process: When choosing the deterministic warp time $\mathcal{M}(t) = t$ we have $T_\mathcal{M}(q) = q - 1$ since $S_\mathcal{M}^n(q) = 2^n \cdot 2^{-nq}$ for all n. Also, $\mathcal{V} = V$. We obtain $T_\mathcal{M}(qH) = qH - 1$ which has to be inserted into (24) to obtain

$$\text{Simple } H\text{-sssi:} \qquad T_V(q) = \begin{cases} qH - 1 & \text{if } \mathbb{E}_\Omega\left[|\sup_{0\le t\le 1} V(t)|^q\right] < \infty \\ -\infty & \text{else.} \end{cases} \tag{25}$$

1.5.3 Local analysis of warped fBm

Let us now turn to the special case where V is fBm. Then, we use the term FB(MF) to abbreviate *fractional Brownian motion in multifractal time*: $\mathcal{B}(t) = B_H(\mathcal{M}(t))$. First, to obtain an intuition on what to expect from the spectra of $\mathcal{B}$ let us note that the moments appearing in (24) are finite for all q due to lemma 34. Applying the Legendre transform yields easily that

$$T_\mathcal{B}^*(a) = \inf_q (qa - T_\mathcal{M}(qH)) = T_\mathcal{M}^*(a/H). \tag{26}$$

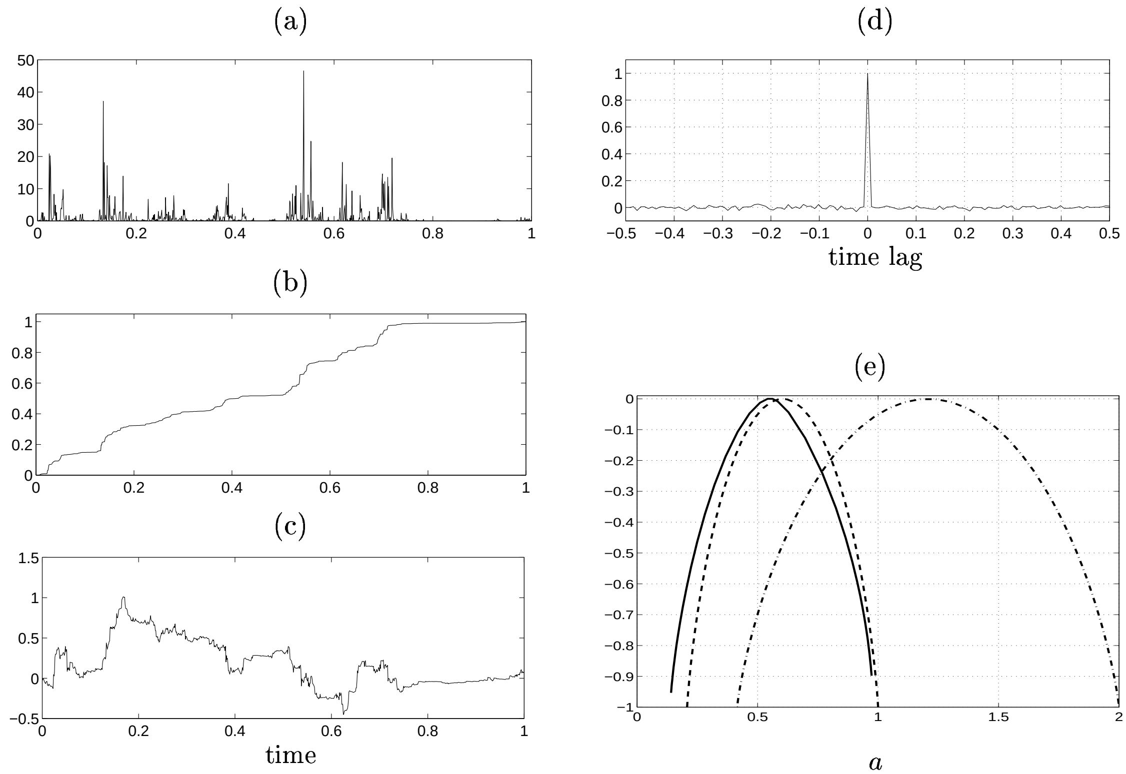

Figure 3: *Left: Simulation of Brownian motion in binomial time (a) Sampling of* $\mathcal{M}_b((k+1)2^{-n}) - \mathcal{M}_b(k2^{-n})$ $(k = 0, \dots, 2^n - 1)$*, indicating distortion of dyadic time intervals (b)* $\mathcal{M}_b((k2^{-n}))$*: the time warp (c) Brownian motion warped with (b):* $\mathcal{B}(k2^{-n}) = B_{1/2}(\mathcal{M}_b(k2^{-n}))$
Right: Estimation of $\dim E_a^{\mathcal{B}}$ *via* $\tau^*_{w,\mathcal{B}}$ *(d) Empirical correlation of the Haar wavelet coefficients. (e) Dot-dashed:* $T^*_{\mathcal{M}_b}$ *(from theory), dashed:* $T^*_{\mathcal{B}}(a) = T^*_{\mathcal{M}_b}(a/H)$ *Solid: the estimator* $\tau^*_{w,\mathcal{B}}$ *obtained from (c). (Reproduced from [32].)*

Second, towards the local analysis we recall the uniform and strict Hölder continuity of the paths of fBm[5] which reads roughly as

$$\sup_{|u|\le\delta} |\mathcal{B}(t+u) - \mathcal{B}(t)| = \sup_{|u|\le\delta} |B_H(\mathcal{M}(t+u)) - B_H(\mathcal{M}(t))| \simeq \sup_{|u|\le\delta} |\mathcal{M}(t+u) - \mathcal{M}(t)|^H.$$

This is the key to conclude that B_H simply squeezes the Hölder regularity exponents by a factor H. Thus,

$$\underline{h}_{\mathcal{B}}(t) = H \cdot \underline{h}_{\mathcal{M}}(t), \qquad E^{\mathcal{M}}_{a/H} = E^{\mathcal{B}}_a,$$

and, consequently, analogous to (26),

$$\boxed{d_{\mathcal{B}}(a) = d_{\mathcal{M}}(a/H).}$$

[5]See theorem 33 for precise statement due to Adler [4].

Figure 3 (d)-(e) displays an estimation of $d_{\mathcal{B}}(a)$ using wavelets which agrees very closely with the form $d_{\mathcal{M}}(a/H)$ predicted by theory. (For statistics on this estimator see [32, 33].)

In conclusion:

Corollary 2 (Fractional Brownian Motion in Multifractal Time) *Let B_H denote fBm of Hurst parameter H. Let $\mathcal{M}(t)$ be of almost surely continuous paths and independent of B_H. Then,* **the multifractal warp formalism**

$$\boxed{\dim(E_a^{\mathcal{B}}) = f_{\mathcal{B}}(a) = \tau_{\mathcal{B}}^*(a) = T_{\mathcal{B}}^*(a) = T_{\mathcal{M}}^*(a/H)} \tag{27}$$

holds for $\mathcal{B}(t) = B_H(\mathcal{M}(t))$ for any a for which $\dim(E_{a/H}^{\mathcal{M}}) = T_{\mathcal{M}}^*(a/H)$.

This means that the local, or fine, multifractal structure of $\mathcal{B}$ captured in $\dim(E_a^{\mathcal{B}})$ on the left can be estimated through grain based, simpler and numerically more robust spectra on the right side, such as $\tau_{\mathcal{B}}^*(a)$ (compare Figure 3 (e)).

The 'warp formula' (27) is appealing since it allows to *separate* the LRD parameter of fBm and the multifractal spectrum of the time change $\mathcal{M}$ given $T_{\mathcal{B}}^*$. Indeed, provided that $\mathcal{M}$ is almost surely increasing one has $T_{\mathcal{M}}(1) = 0$ since $S^n(0) = \mathcal{M}(1)$ for all n. Thus, $T_{\mathcal{B}}(1/H) = 0$ exposes the value of H. Alternatively, the tangent at $T_{\mathcal{B}}^*$ through the origin has slope $1/H$. Once H is known $T_{\mathcal{M}}^*$ follows easily from $T_{\mathcal{B}}^*$.

Simple fBm: When choosing the deterministic warp time $\mathcal{M}(t) = t$ we have $\mathcal{B} = B_H$ and $T_{\mathcal{M}}(q) = q - 1$ since $S_{\mathcal{M}}^n(q) = 2^n \cdot 2^{-nq}$ for all n. We conclude that

$$T_{B_H}(q) = qH - 1 \tag{28}$$

for all q. This confirms (19) for fGn. With (27) it shows that all spectra of fBm consist of the one point $(H, 1)$ only, making the mono-fractal character of this process most explicit.

1.5.4 LRD and estimation of warped fBm

Let $\mathcal{G}(k) := \mathcal{B}((k+1)2^{-n}) - \mathcal{B}(k2^{-n})$ be fGn in multifractal time (see (22) for the case $H = 1/2$). Calculating auto-correlations explicitly, lemma 41 shows that $\mathcal{G}$ is second order stationary under mild conditions with

$$H_{\mathcal{G}} = \frac{T_{\mathcal{M}}(2H) + 1}{2}. \tag{29}$$

Let us discuss some special cases. For a continuous, increasing warp time $\mathcal{M}$, e.g., we have always $T_{\mathcal{M}}(0) = -1$ and $T_{\mathcal{M}}(1) = 0$. Exploiting the concave shape of $T_{\mathcal{M}}$ we find that $H < H_{\mathcal{G}} < 1/2$ for $0 < H < 1/2$, and $1/2 < H_{\mathcal{G}} < H$ for $1/2 < H < 1$. Thus, multifractal warping can not create LRD and it seems to weaken the dependence as measured through second order statistics.

Especially in the case of $H = 1/2$ ('white noise in multifractal time') $\mathcal{G}(k)$ becomes *uncorrelated*. This follows from (173). Notably, this is a stronger statement than the observation that the $\mathcal{G}(k)$ are *independent conditioned* on $\mathcal{M}$ (compare Section 1.5.1). As a particular consequence, wavelet coefficients will decorrelate fast for the entire process $\mathcal{G}$, not only when conditioning on $\mathcal{M}$ (compare Figure 3 (d)). This is favorable for estimation purposes as it reduces the error variance.

Of larger importance, however, is the warning that the vanishing correlations should not make one conclude on independence of $\mathcal{G}(k)$. After all, $\mathcal{G}$ becomes Gaussian only when conditioning on knowing $\mathcal{M}$. A strong, higher order dependence in $\mathcal{G}$ is hidden in the dependence of the increments of $\mathcal{M}$ which determine the variance of $\mathcal{G}(k)$ as in (22). Indeed, Figure 3 (c) shows clear phases of monotony of $\mathcal{B}$ indicating positive dependence in its increments $\mathcal{G}$, despite vanishing correlations. Mandelbrot calls this the 'blind spot of spectral analysis'.

1.5.5 Multifractals in multifractal time

Despite of its simplicity the presented scheme for constructing multifractal processes allows for various play-forms some of which are little explored. First of all, for simulation purposes one might subject the *randomized Weierstrass-Mandelbrot function* to time change rather than fBm itself.

Next, we may choose to replace fBm with a more general self-similar process (130) such as stable motion. Difficulties arise here since Levy motion is itself a multifractal with varying Hölder regularity and the challenge lies in studying which exponents of the 'multifractal time' and the motion are most likely to meet. A solution for the spectrum $f(a)$ is given in corollary 43 which actually applies to arbitrary processes Y with stationary increments (compare theorem 44) replacing fBm. In its most compact form our result gives the multifractal spectrum of $\mathcal{Y} := Y(\mathcal{M})$ through $f_{\mathcal{Y}}(a) = T^*_{\mathcal{Y}}(a)$ where

$$\boxed{T_{\mathcal{Y}}(q) = T_{\mathcal{M}}\Big(T_Y(q) + 1\Big)\ .}$$

In the special case when Y is almost surely increasing, i.e. a multifractal in the classical sense, a close connection to the so-called 'relative multifractal analysis' [71] can be established using the concept of inverse multifractals [70]: understanding the multifractal structure of $\mathcal{Y}$ is equivalent to knowning the multifractal spectra of Y with respect to $\mathcal{M}^{-1}$, the inverse function of $\mathcal{M}$. We will show how this can be resolved in the simple case of Binomial cascades.